

QC944

N39

no. 70

ATSL

NATIONAL HURRICANE RESEARCH PROJECT

N39

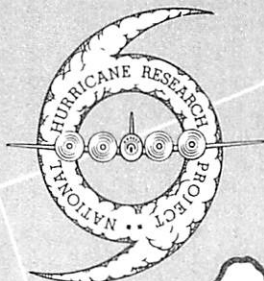
no. 70

ATSL

REPORT NO. 70

Some Theoretical Results Which Pertain to the Upper-Tropospheric Vortex Trains of the Tropics

ATMOSPHERIC SCIENCE
LABORATORY COLLECTION



U. S. DEPARTMENT OF COMMERCE

Luther H. Hodges, Secretary

WEATHER BUREAU

Robert M. White, Chief

ATMOSPHERIC SCIENCE
LABORATORY COLLECTION

NATIONAL HURRICANE RESEARCH PROJECT

REPORT NO. 70

Some Theoretical Results Which
Pertain to the Upper-Tropospheric
Vortex Trains of the Tropics

by

Stanley L. Rosenthal

National Hurricane Research Project, Miami, Fla.



Washington, D. C.

April 1964



U18401 0601264

NATIONAL HURRICANE RESEARCH PROJECT REPORTS

Reports by Weather Bureau units, contractors, and cooperators working on the hurricane problem are preprinted in this series to facilitate immediate distribution of the information among the workers and other interested units. As this limited reproduction and distribution in this form do not constitute formal scientific publication, reference to a paper in the series should identify it as a preprinted report.

- No. 1. Objectives and basic design of the NHRP. March 1956.
- No. 2. Numerical weather prediction of hurricane motion. July 1956.
Supplement: Error analysis of prognostic 500-mb. maps made for numerical weather prediction of hurricane motion. March 1957.
- No. 3. Rainfall associated with hurricanes. July 1956.
- No. 4. Some problems involved in the study of storm surges. December 1956.
- No. 5. Survey of meteorological factors pertinent to reduction of loss of life and property in hurricane situations. March 1957.
- No. 6. A mean atmosphere for the West Indies area. May 1957.
- No. 7. An index of tide gages and tide gage records for the Atlantic and Gulf coasts of the United States. May 1957.
- No. 8. Part I. Hurricanes and the sea surface temperature field. Part II. The exchange of energy between the sea and the atmosphere in relation to hurricane behavior. June 1957.
- No. 9. Seasonal variations in the frequency of North Atlantic tropical cyclones related to the general circulation. July 1957.
- No. 10. Estimating central pressure of tropical cyclones from aircraft data. August 1957.
- No. 11. Instrumentation of National Hurricane Research Project aircraft. August 1957.
- No. 12. Studies of hurricane spiral bands as observed on radar. September 1957.
- No. 13. Mean soundings for the hurricane eye. September 1957.
- No. 14. On the maximum intensity of hurricanes. December 1957.
- No. 15. The three-dimensional wind structure around a tropical cyclone. January 1958.
- No. 16. Modification of hurricanes through cloud seeding. May 1958.
- No. 17. Analysis of tropical storm Frieda 1957. A preliminary report. June 1958.
- No. 18. The use of mean layer winds as a hurricane steering mechanism. June 1958.
- No. 19. Further examination of the balance of angular momentum in the mature hurricane. July 1958.
- No. 20. On the energetics of the mature hurricane and other rotating wind systems. July 1958.
- No. 21. Formation of tropical storms related to anomalies of the long-period mean circulation. September 1958.
- No. 22. On production of kinetic energy from condensation heating. October 1958.
- No. 23. Hurricane Audrey storm tide. October 1958.
- No. 24. Details of circulation in the high energy core of hurricane Carrie. November 1958.
- No. 25. Distribution of surface friction in hurricanes. November 1958.
- No. 26. A note on the origin of hurricane radar spiral bands and the echoes which form them. February 1959.
- No. 27. Proceedings of the Board of Review and Conference on Research Progress. March 1959.
- No. 28. A model hurricane plan for a coastal community. March 1959.
- No. 29. Exchange of heat, moisture, and momentum between hurricane Ella (1958) and its environment. April 1959.
- No. 30. Mean soundings for the Gulf of Mexico area. April 1959.
- No. 31. On the dynamics and energy transformations in steady-state hurricanes. August 1959.
- No. 32. An interim hurricane storm surge forecasting guide. August 1959.
- No. 33. Meteorological considerations pertinent to standard project hurricane, Atlantic and Gulf coasts of the United States. November 1959.
- No. 34. Filling and intensity changes in hurricanes over land. November 1959.
- No. 35. Wind and pressure fields in the stratosphere over the West Indies region in August 1958. December 1959.
- No. 36. Climatological aspects of intensity of typhoons. February 1960.
- No. 37. Unrest in the upper stratosphere over the Caribbean Sea during January 1960. April 1960.
- No. 38. On quantitative precipitation forecasting. August 1960.
- No. 39. Surface winds near the center of hurricanes (and other cyclones). September 1960.
- No. 40. Surface winds near the center of hurricanes (and other cyclones). September 1960.
- No. 41. On initiation of tropical depressions and convection in a conditionally unstable atmosphere. October 1960.
- No. 42. On the heat balance of the troposphere and water body of the Caribbean Sea. December 1960.
- No. 43. Climatology of 24-hour North Atlantic tropical cyclone movements. January 1961.
- No. 44. Climatology of 24-hour North Atlantic tropical cyclone movements. January 1961.
- No. 45. Prediction of movements and surface pressures of typhoon centers in the Far East by statistical methods. May 1961.
- No. 46. Marked changes in the characteristics of the eye of intense typhoons between the deepening and filling states. May 1961.
- No. 47. The occurrence of anomalous winds and their significance. June 1961.
- No. 48. Some aspects of hurricane Daisy, 1958. July 1961.
- No. 49. Concerning the mechanics and thermodynamics of the inflow layer of the mature hurricane. September 1961.
- No. 50. On the structure of hurricane Daisy (1958). October 1961.
- No. 51. Concerning the mechanics and thermodynamics of the inflow layer of the mature hurricane. September 1961.
- No. 52. On the structure of hurricane Daisy (1958). October 1961.
- No. 53. Some properties of hurricane wind fields as deduced from trajectories. November 1961.
- No. 54. Proceedings of the Second Technical Conference on Hurricanes, June 27-30, 1961, Miami Beach, Fla. March 1962.
- No. 55. Concerning the general vertically averaged hydrodynamic equations with respect to basic storm surge equations. April 1962.
- No. 56. Inventory, use, and availability of NHRP meteorological data gathered by aircraft. April 1962.
- No. 57. On the momentum and energy balance of hurricane Helene (1958). April 1962.
- No. 58. On the balance of forces and radial accelerations in hurricanes. June 1962.
- No. 59. Vertical wind profiles in hurricanes. June 1962.
- No. 60. A theoretical analysis of the field of motion in the hurricane boundary layer. June 1962.
- No. 61. On the dynamics of disturbed circulation in the lower mesosphere. August 1962.
- No. 62. Mean sounding data over the western tropical Pacific Ocean during the typhoon season. and Distribution of turbulence and icing in the tropical cyclone. October 1962.
- No. 63. Reconstruction of the surface pressure and wind fields of hurricane Helene. October 1962.
- No. 64. A cloud seeding experiment in hurricane Esther, 1961. November 1962.
- No. 65. Studies on statistical prediction of typhoons. April 1963.
- No. 66. The distribution of liquid water in hurricanes. June 1963.
- No. 67. Some relations between wind and thermal structure of steady state hurricanes. June 1963.
- No. 68. Instability aspects of hurricane genesis. June 1963.
- No. 69. On the evolution of the wind field during the life cycle of tropical cyclones. November 1963.
- No. 70. On the filling of tropical cyclones over land, with particular reference to hurricane Donna of 1960. December 1963.
- No. 71. On the thermal structure of developing tropical cyclones. January 1964.
- No. 72. Criteria for a standard project northeaster for New England north of Cape Cod. March 1964.
- No. 73. A study of hurricane rainbands. March 1964.

QC944
. N39
10.70
ATSL

CONTENTS

	Page
ABSTRACT	1
1. INTRODUCTION	1
2. THE MODEL	3
3. RESULTS	9
Base State A	11
Base State B	11
Base State C	11
Base State D	11
4. CONCLUSIONS	18
ACKNOWLEDGMENT	24
REFERENCES	24
APPENDIX	26

ATSL
10.70
N39
QC944

SOME THEORETICAL RESULTS WHICH PERTAIN TO THE UPPER-TROPOSPHERIC VORTEX TRAINS OF THE TROPICS

Stanley L. Rosenthal

National Hurricane Research Project, U. S. Weather Bureau, Miami, Fla.

ABSTRACT

It is generally assumed that the vortex trains of the upper tropical troposphere are indirect circulations which require an external source of kinetic energy for their maintenance. In this investigation, the linearized, quasi-geostrophic equations were solved numerically as an initial value problem. Several base states, which resemble actual conditions when upper-tropospheric vortex trains exist, were treated. The amplitude of the initial perturbation varied with altitude in a fairly realistic fashion. The phase of the perturbation was initially invariant with altitude. Integrations were carried out to 48 hr. The results indicate that disturbances with wavelengths of, and in excess of, 3000 km. are not damped. This is felt to be evidence opposed to the contention that the tropical vortex trains are indirect circulations.

1. INTRODUCTION

During the warm season, the tropical troposphere may be divided into two distinct layers. The lower of these is 10,000-20,000 ft. thick and is distinguished by the trade winds. The upper troposphere is characterized by a cellular structure of cyclones and anticyclones.¹ These vortices are most intense near 200 mb.² Usually, they are completely contained in the 500-100-mb. layer [5, 8, 10, 14].

Although these upper-tropospheric disturbances may persist for weeks at a time [10, 15], Riehl [16] contends that they are indirect circulations and, hence, must rely on kinetic energy released elsewhere in the atmosphere for their maintenance. Palmer [10, 11] seems to have taken this same point of view. However, irrefutable evidence to support this contention seems to be lacking.³ It is clear from the literature [11, 15, 17], as well as from figure 1, that the lower portion of the tropical troposphere is, in the mean, very nearly barotropic while the upper troposphere is distinctly baroclinic.

¹ These descriptions pertain to the Northern Hemisphere. Although similar phenomena are likely to be found in the Southern Hemisphere, the author is unaware of systematic documentation of such.

² Kona-type lows which are most intense in the middle and low troposphere appear to be of a distinctly different nature than the upper-tropospheric vortices [12, 18]. Kona lows are not discussed in this report.

³ Two empirical studies currently in progress at the National Hurricane Center are concerned with this problem.

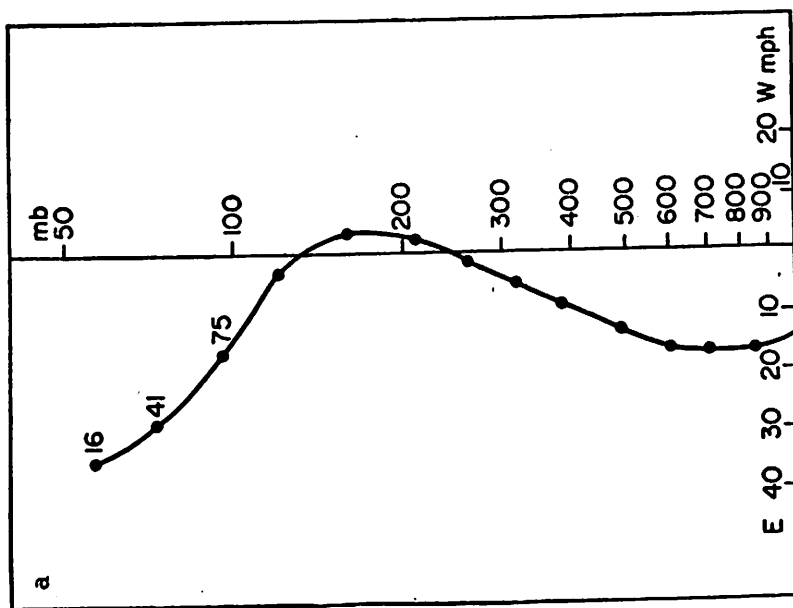
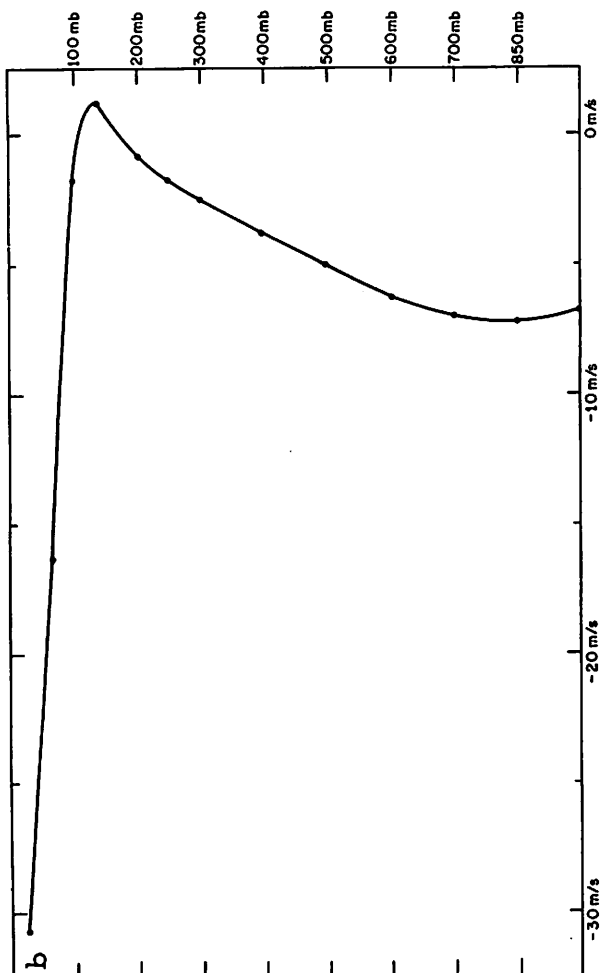


Figure 1. - Mean zonal wind (a) over Tropical Pacific during September 1945 (after Riehl [15]), (b) at Eniwetok in July 1958 (after Yanai [20]).

It is, therefore, not unreasonable to expect that the upper-level vortices are affected by this baroclinicity. Whether this baroclinicity serves as a damping or an amplifying agent has not as yet been determined.

As noted earlier, workers at the National Hurricane Center are currently engaged in empirical studies of these upper-tropospheric vortices. The purpose of this paper is to present some results from a theoretical investigation of the same problem. In view of the complexities involved, the theory is intended to be applicable only under certain special circumstances.

Synoptic experience indicates that it is possible to delineate at least two basically different regimes in the cellular structure of the upper tropical troposphere. Broadly speaking, the first of these regimes may be pictured as one in which the 200-mb. systems are arranged in a more or less chaotic pattern and there exists considerable relative motion between the various centers. The general impression received from the study of a sequence of such charts is that of confusion.

In contrast to this chaotic regime is the simpler situation first described by Riehl [15, 17]. In this case, we have a train of regularly spaced, alternating cyclones and anticyclones. The centers of these systems are typically at a latitude of about 20°N. and their north-south extent is roughly 20° of latitude. During the period studied by Riehl [15, 17], spacing between consecutive cyclones (or anticyclones) was about 45° of longitude. (or roughly 4710 km.) Synoptic experience shows that the spacing is often less than this amount and, at times, somewhat greater. If middle-latitude systems do not penetrate into the Tropics, these vortex trains can exist for several weeks with steady westward progression of the cells. Riehl [17] suggests that such a vortex train can be thought of as "a train of waves in air with zero basic current so that the perturbations appear as closed circulations." The remainder of this paper pertains only to this wave-like regime.

2. THE MODEL

Despite difficulties near the equator, assumptions of gradient or geostrophic wind balance have often proved fruitful when applied to the so-called "sub-tropical" latitudes [4, 6, 11, 17]. The disturbances considered in this paper exist for long periods of time with only small changes in intensity. Under such circumstances, one would expect the wind and pressure fields to be very nearly in balance. Also, scale theory [2] predicts that the balance equation [3] should be a valid approximation in low latitudes provided that the disturbances are of synoptic scale and the motion is nonviscous and adiabatic. In the balance equation, however, centrifugal effects are represented by terms which are nonlinear in the stream function. If this equation is linearized in the usual manner and if the basic (zonal) current is invariant in the meridional direction, these higher-order terms will vanish. In view of this, simple geostrophic motion was assumed in the construction of our model. It is recognized that the neglect of centrifugal effects may limit the utility of the results. Viscous and diabatic effects have also been neglected.

With the geostrophic approximation,

$$\mathbf{w} = (\hat{k}/f_0) \times \nabla \phi \quad (1)$$

the energetically consistent vorticity and thermodynamic equations are [1], respectively,

$$\frac{\partial \zeta}{\partial t} + \mathbf{V} \cdot \nabla (f + \zeta) = f_0 \frac{\partial \omega}{\partial p}, \quad (2)$$

$$\frac{\partial^2 \phi}{\partial p \partial t} + \mathbf{V} \cdot \nabla \frac{\partial \phi}{\partial p} + \sigma \omega = 0, \quad (3)$$

where

$$\sigma = \theta^{-1} \frac{\partial \theta}{\partial p} \frac{\partial \theta}{\partial p} \quad (4)$$

is the static stability (taken to be, at most, a function of only pressure), f_0 is a standard value of the Coriolis parameter, $\zeta = f_0^{-1} \nabla^2 \phi$; the remaining notation is standard. The variables, ϕ , \mathbf{V} and ω , are written

$$\phi = \bar{\phi}(p, y) + \phi'(x, y, p, t) \quad (5)$$

$$\mathbf{V} = U(p) \hat{i} + \mathbf{V}'(x, y, p, t) \quad (6)$$

and

$$\omega = \omega'(x, y, p, t) \quad (7)$$

where the primes denote perturbation quantities. $\bar{\phi}(p, y)$ is the geopotential of the base state; $U(p)$ is the mean zonal wind; \hat{i} is a unit vector pointing eastward; x is east-west distance; y is north-south distance. From equation (1),

$$U(p) = -\frac{1}{f_0} \frac{\partial \bar{\phi}}{\partial y} \quad (8)$$

Proceeding in a routine fashion, we linearize equations (2) and (3) to obtain

$$\nabla^2 \frac{\partial \phi'}{\partial t} + U \nabla^2 \frac{\partial \phi'}{\partial x} + \beta \frac{\partial \phi'}{\partial x} = f_0^2 \frac{\partial \omega'}{\partial p} \quad (9)$$

and

$$\frac{\partial^2 \phi'}{\partial p \partial t} + U \frac{\partial^2 \phi'}{\partial p \partial x} - \frac{dU}{dp} \frac{\partial \phi'}{\partial x} + \sigma \omega' = 0 \quad (10)$$

The ω -equation for the problem is obtained by eliminating time derivatives between equations (9) and (10). This gives

$$\sigma \nabla^2 \omega' + f_0^2 \frac{\partial^2 \omega'}{\partial p^2} = 2 \frac{dU}{dp} \nabla^2 \frac{\partial \phi'}{\partial x} + \beta \frac{\partial^2 \phi'}{\partial p \partial x} \quad (11)$$

Equations (9) and (11), with suitable side conditions, form a complete mathematical system for the dependent variables ϕ' and ω' .

Following along lines similar to Wiin-Nielsen's study of waves in the westerlies [19], we assume solutions of the form

$$\phi' = \cos my [A(p, t) \sin kx + B(p, t) \cos kx], \quad (12)$$

$$\omega' = \cos my [C(p, t) \sin kx + D(p, t) \cos kx]. \quad (13)$$

Alternately, we may write

$$\phi' = R_1 \cos my \cos (kx + \delta_1),$$

$$\omega' = R_2 \cos my \cos (kx + \delta_2),$$

where $R_1 = (A^2 + B^2)^{1/2}$, $\tan \delta_1 = A/B$, $R_2 = (C^2 + D^2)^{1/2}$, $\tan \delta_2 = C/D$. R_1 and R_2 are, respectively, the amplitudes of the geopotential- and vertical-motion perturbations. The quantities δ_1 and δ_2 are, respectively, the phase angles of the geopotential- and vertical-motion perturbations.

Smooth walls are assumed at $y = \pm \pi/2m$; the origin of the y -axis is the central latitude (20°) of the wave train. As noted in the previous section, the vortex-train (or wave-like) regime persists only when a well-marked, nearly stationary boundary exists between the circulations of the low and middle latitudes. The smooth wall concept, embodied in equations (12) and (13) would, therefore, seem to be realistic for this particular regime.

The field of perturbation geopotential, described by equation (12), when projected onto isobaric surfaces is composed of closed cells (although certainly not circular ones). The field of total geopotential, $\phi = \bar{\phi} + \phi'$, will also show closed cells on isobaric surfaces where the basic zonal current, $U(p)$, is relatively weak. On other isobaric surfaces, where $U(p)$ is relatively strong, the total geopotential will appear as open waves of finite meridional extent.

No assumption will be made concerning the time dependence of the coefficients A , B , C , and D . The mathematical task is not, therefore, the solution of an eigen value problem. Instead, a sequence of initial value problems are solved. Differences between the philosophies of the eigen value and initial value approaches to the treatment of linearized meteorological equations have been discussed by Wiin-Nielsen [19]. We will not repeat his discourse here.

When equations (12) and (13) are substituted into (9) and (11), and coefficients of $\sin kx$ and $\cos kx$ are equated, one obtains

$$\frac{\partial A}{\partial t} = kc_R B - \left(\frac{f_0}{n}\right)^2 \frac{\partial C}{\partial p}, \quad (14)$$

$$\frac{\partial B}{\partial t} = -kc_R A - \left(\frac{f_0}{n}\right)^2 \frac{\partial D}{\partial p}, \quad (15)$$

$$\frac{\partial^2 C}{\partial p^2} - \sigma \left(\frac{n}{f_0}\right)^2 C = 2k \left(\frac{n}{f_0}\right)^2 \frac{dU}{dp} B - \frac{\beta k}{f_0^2} \frac{\partial B}{\partial p}, \quad (16)$$

and

$$\frac{\partial^2 D}{\partial p^2} - \sigma \left(\frac{n}{f_0}\right)^2 D = -2k \left(\frac{n}{f_0}\right)^2 \frac{dU}{dp} A + \frac{\beta k}{f_0^2} \frac{\partial A}{\partial p} \quad (17)$$

where

$$n^2 = k^2 + m^2 \quad (18)$$

and

$$c_R = U - \frac{\beta}{n^2} \quad (19)$$

Equations (14)-(17) are very nearly the same as those treated by Wiin-Nielsen [19]. Given initial values of A and B, initial values of C and D may be determined from (16) and (17). A and B, at the next time step, may then be obtained from (14) and (15).

The analog to the subtropical atmosphere which we have created consists of a channel of infinite zonal extent bounded in the meridional direction by smooth vertical walls which are separated by a distance of π/m . Within this channel there exists wave motion of a nonviscous, adiabatic, quasi-geostrophic atmosphere. The perturbation kinetic energy per wavelength is given by

$$K = \frac{1}{2gf_0^2} \int_0^{p_0} \int_0^L \int_{-\pi/2m}^{\pi/2m} \left[\left(\frac{\partial \phi'}{\partial x}\right)^2 + \left(\frac{\partial \phi'}{\partial y}\right)^2 \right] \delta y \delta x \delta p \quad (20)$$

which, by use of (12), may be written

$$K = \frac{(\pi n/f_0)^2}{4gkm} \int_0^{p_0} (A^2 + B^2) \delta p. \quad (21)$$

The quantity p_0 is 1000 mb. and L is the wavelength ($L = 2\pi/R$). The time derivative of (21) is

$$\frac{\partial K}{\partial t} = \frac{(\pi n/f_0)^2}{2gkm} \int_0^{p_0} \left(A \frac{\partial A}{\partial t} + B \frac{\partial B}{\partial t} \right) \delta p. \quad (22)$$

By use of equations (14), (15) and (22), we obtain

$$\frac{\partial K}{\partial t} = - \frac{\pi^2}{2gkm} \int_0^{p_0} \left[A \frac{\partial C}{\partial p} + B \frac{\partial D}{\partial p} \right] \delta p. \quad (23)$$

The boundary conditions, $\omega = 0$ at $p = 0$ and $p = p_0$, require $C = D = 0$ at $p = 0$ and $p = p_0$. By use of these conditions and equation (23), we obtain

$$\frac{\partial K}{\partial t} = \frac{\pi^2}{2gkm} \int_0^{p_0} \left[C \frac{\partial A}{\partial p} + D \frac{\partial B}{\partial p} \right] \delta p. \quad (24)$$

Within the framework of equation (12), disturbances with vertical axes may be represented by the requirement that the phase of the ϕ' -disturbance be the same at all pressures. Since the origin of the x-axis is arbitrary, ϕ' for such a disturbance may be written

$$\phi' = A \cos my \sin kx \quad (25a)$$

$$B = 0 \quad (25b)$$

When these relationships are valid, equation (16), along with the boundary conditions on C , can be satisfied only in the trivial case $C \equiv 0$. By use of this result and of equation (25b), we obtain from equation (24), $\partial K/\partial t = 0$. For this case, the vertical-motion patterns are 90° or 270° out of phase with the fields of geopotential and temperature. As a result, ascending and descending air have the same temperature and there is no net generation of kinetic energy. Similar conclusions for disturbances with vertical axes have been obtained from many other studies. This result is not restricted to linear models.

In the nonlinear case, the ω -equation may be written

$$\sigma \nabla^2 \omega + f_0^2 \frac{\partial^2 \omega}{\partial p^2} = f_0 \frac{\partial}{\partial p} (\mathbf{V} \cdot \nabla (f + \zeta)) - \nabla^2 (\mathbf{V} \cdot \nabla \frac{\partial \phi}{\partial p}) \quad (26)$$

To represent nonsloping wave disturbances superimposed on a zonal current which varies only with pressure, we may write

$$\phi = -f_0 y U(p) + f_0 H(p) \cos my \sin kx \quad (27)$$

where $H(p)$ is an amplitude factor. Substitution of (27) into (26) gives

$$\sigma \nabla^2 \omega + f_0^2 \frac{\partial^2 \omega}{\partial p^2} = f_0 k \left[\beta \frac{dH}{dp} - 2n^2 H \frac{dU}{dp} \right] \cos kx \cos my \quad (28)$$

Equation (28) has solutions of the form

$$\omega = F(p) \cos my \cos kx \quad (29)$$

where $F(p)$ is the solution of

$$\frac{d^2 F}{dp^2} - \left(\frac{n}{f_0} \right)^2 \sigma F = \frac{k}{f_0} \left[\beta \frac{dH}{dp} - 2n^2 H \frac{dU}{dp} \right] \quad (30)$$

which satisfies the boundary conditions $F = 0$ at $p = 0$ and $p = p_0$. The rate per wavelength at which potential energy is converted into kinetic energy in the nonlinear model described by equations (1), (2), and (3) may be shown to be proportional to

$$\int_0^{p_0} \int_{-\pi/2m}^{\pi/2m} \int_0^L \omega \frac{\partial \phi}{\partial p} \delta x \delta y \delta p$$

This integral vanishes when ϕ and ω are given by equations (27) and (29), respectively. As was found in the linear case, the field of vertical motion is 90° or 270° out of phase with the geopotential and temperature fields.

This result is of significance in the selection of initial conditions for our calculation because the author has been unable to locate evidence concerning a slope with height of the axes of the upper-tropospheric vortices. Even in a rather careful study of composite data for six of the upper-tropospheric cyclones [14], there is no mention of such slopes. Despite Rick's fine piece of work [14], we can hardly take the point of view that the upper-tropospheric vortices have been completely described and that the vortex axes are indeed vertical. At this point we are faced with one of the major weaknesses of the initial value (as compared to the eigen value) approach. If the eigen value problem could be solved, the solutions would yield the complete structure of the disturbances for any amplifying, decaying, or neutral modes that might exist. In the initial value problem, the initial structure of the disturbances must be specified from our empirical knowledge and, in this case, our knowledge is limited.

In an application of the initial value approach to waves in the west-lies, Wiin-Nielsen [19] employed initial conditions in which the phase angles and amplitudes of the ϕ -waves were invariant with height. His results showed that the disturbances quickly developed slopes, and decayed or amplified depending on wavelength. It would seem that a reasonable approach to the problem of the upper-tropospheric vortices would be to postulate initial disturbances whose ϕ' -amplitudes vary with pressure in a manner which resembles the observed variation and whose ϕ' -phase is constant. The changes with time of these systems could then be examined for various wavelengths and realistic base states. In particular, we would seek to discover whether or not the initial perturbations evolve into damped disturbances at wavelengths which approximate the observed spacing between consecutive cyclones (or anticyclones). If this were to occur, it would seem to be evidence in support of the contention that the upper-tropospheric vortex trains do indeed require an external source of kinetic energy for their maintenance. On the other hand, if the integrations were to yield amplifying or neutral systems, this would seem to support the contention that the upper-tropospheric vortex trains can maintain themselves in the absence of an external source of kinetic energy.

Our solutions of equations (14)-(17) are discussed in the next section. Information concerning the numerical methods used to obtain the solutions is found in the appendix.

3. RESULTS

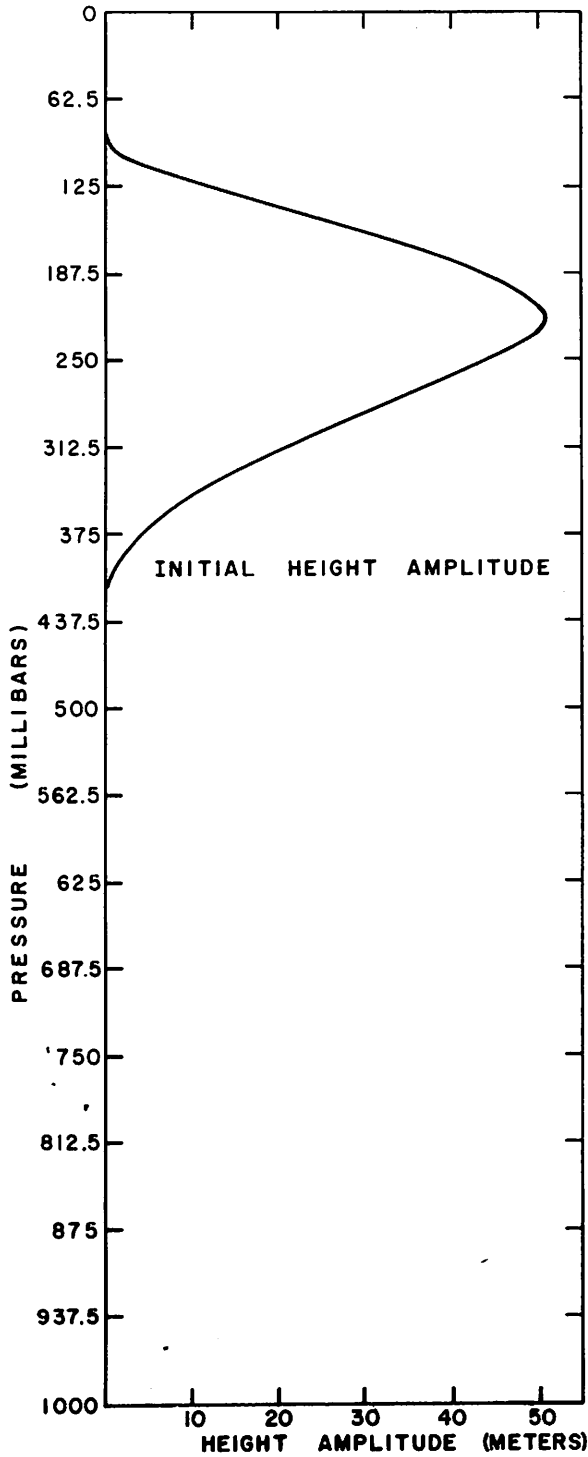
Figure 2 shows the function selected to portray the initial distribution of z' -amplitude ($z' = \phi'/g$). The pressure scale shows full tick marks at every second grid point and half-tick marks at the intermediate points. The amplitude is at a maximum at 218.75 mb. and vanishes at 93.75 and 406.25 mb. This function is based on our rather meager empirical knowledge of the upper-tropospheric vortices.

Since the upper-tropospheric vortices are not observed to reach the 100 mb. surface, the initial z' -amplitude vanishes at 93.75 mb. which is the pressure of the grid point closest to 100 mb. Experience indicates that these disturbances usually do not extend below 400 mb. For this reason, the initial z' -amplitude was forced to zero at the 406.25-mb. grid point.

We can be reasonably sure that the gross aspects of figure 2 (a maximum of amplitude close to 200 mb., with this parameter going to 0 near 100 and 400 mb.) are fairly realistic; the details of the curve are, however, entirely speculative. It should be noted that our results are valid for any distribution of initial z' -amplitude which can be obtained by scaling the curve shown in figure 2 by a constant multiplier. Of course, the results must then also be scaled by the same multiplier.

In each case, the integrations covered a 48-hr. period. Jordan's data [7] were used to calculate the distribution of static stability employed in the computations (see table 1). The Coriolis parameter, f_0 , and β were evaluated for 20° N. The parameter m was selected so that the half-width of the channel was 10° of latitude. Four base states were treated. The first of these was a constant (barotropic) zonal current of 7 m. sec.⁻¹ This current is

Table 1. - Static stability as a function of pressure. Values are computed from Jordan's data [7].



Pressure	Index	(m ² sec. ⁻² cb. ⁻²)
0	1	
31.25	2	2400
62.50	3	540
93.75	4	275
125.00	5	105
156.25	6	31.5
187.50	7	10.5
218.75	8	7.9
250.00	9	5.39
281.25	10	5.30
312.50	11	5.05
343.75	12	4.76
375.00	13	4.45
406.25	14	4.18
437.50	15	3.90
468.75	16	3.60
500.00	17	3.30
531.25	18	3.20
562.50	19	3.07
593.75	20	2.95
625.00	21	2.45
656.25	22	1.97
687.50	23	1.90
718.75	24	1.82
750.00	25	1.75
781.25	26	1.69
812.50	27	1.61
843.75	28	1.53
875.00	29	1.45
906.25	30	1.37
937.50	31	1.30
968.75	32	1.24
1000	33	

Figure 2. - Vertical profile of initial z'-amplitude

referred to as "Base State A". Three baroclinic currents, shown by figure 3, and referred to, respectively, as "Base States B, C, and D" were also treated. For each of these base states, the wavelength was varied from 2,000 to 10,000 km. at 1000-km. intervals.

To obtain preliminary gross estimates of the changes of perturbation intensity, changes of perturbation kinetic energy (the quantity K given by equation (20)) have been examined. While this is a useful parameter, it can not, for our purposes, be the sole measure of intensity. Although deterioration of the upper-tropospheric systems must effect a decrease in K , an increase, or no change, of K could result if the upper-tropospheric systems decayed while systems formed at other levels. Thus, to draw definite conclusions, the data on changes of K must be supplemented by data illustrating changes in structure of the systems. This will be done later.

Base State A: The barotropic base state was included to serve as a control on the baroclinic cases. At the end of 48 hr., no detectable change in K at any wavelength had occurred.

Base State B: This current (fig. 3a) closely resembles the mean zonal wind for Eniwetok during July of 1958 (see fig. 1b). The 48-hr. changes of K are illustrated by the curve marked "Base State B" on figure 4. K increases by about 1 percent for $L = 3000$ and 4000 km. At all other wavelengths, a small decrease in K occurs. Although these changes in K are negligibly small, especially in view of the crudeness of the model, the fact that K increases for wavelengths close to those in which these systems are observed to occur is encouraging.

Base State C: This current (fig. 3b) is similar to Base State B with the exception that the low-level easterlies are 4 m. sec.^{-1} greater and the upper-tropospheric baroclinicity is somewhat stronger. The curve marked "Base State C" on figure 4 shows the 48-hr. changes of K . Again, a decrease of K is found only for $L = 2000$ km. K increases at all other wavelengths. Largest increases again occur at $L = 3000$ and 4000 km.

Base State D: In this case (fig. 3c), the low-level easterlies are 12 m. sec.^{-1} . In the layer 1000-500 mb. The layer 500-156.25 mb. is considerably more baroclinic than in the two previous cases. Again, all wavelengths treated, with the exception of 2000 km., show increases of K . At $L = 2000$ km., K has decreased by about 9 percent. The maximum increase of K , about 18 percent, occurs at $L = 4000$ km.

Distributions of the z' -amplitudes and phase angles at 48 hr. for Base State A, $L = 3000$ km. are shown by figure 5. Similar diagrams for Base States B-D at the wavelength of greatest increase of K are shown, respectively, by figures 6-8. On each of these diagrams, the dashed curve is the initial z' -amplitude. As these curves show, the upper-tropospheric wave trains have induced weak perturbations in the lower troposphere and, also, in the stratosphere. The main features of the initial distribution of z' -amplitude are, however, preserved through the 48-hr. period. It is also clear that the increases of K largely reflect the initiation of new perturbations and not an intensification of the upper-tropospheric disturbance. This is true not only of the cases shown by figures 6-8 but for all cases in which K increased. For

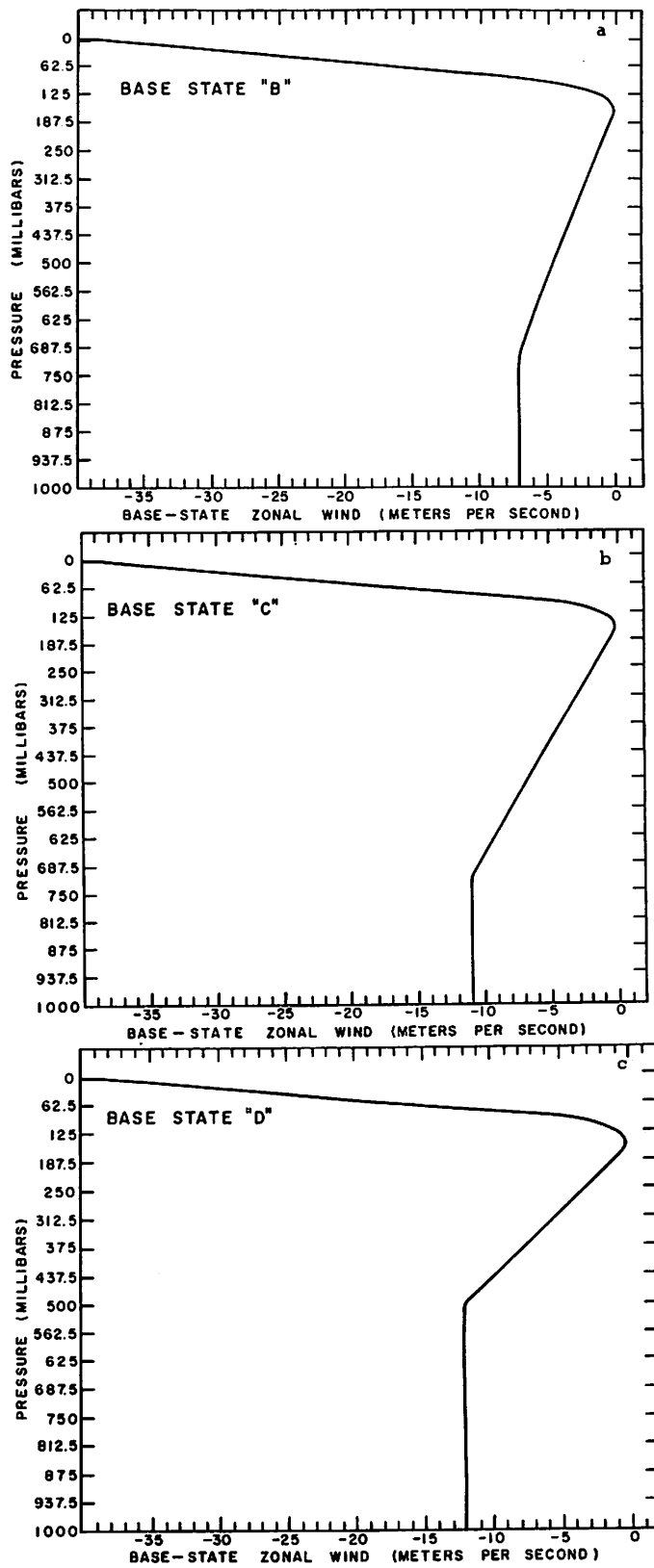


Figure 3. - Hypothetical mean zonal winds (a) Base State B, (b) Base State C, (c) Base State D.

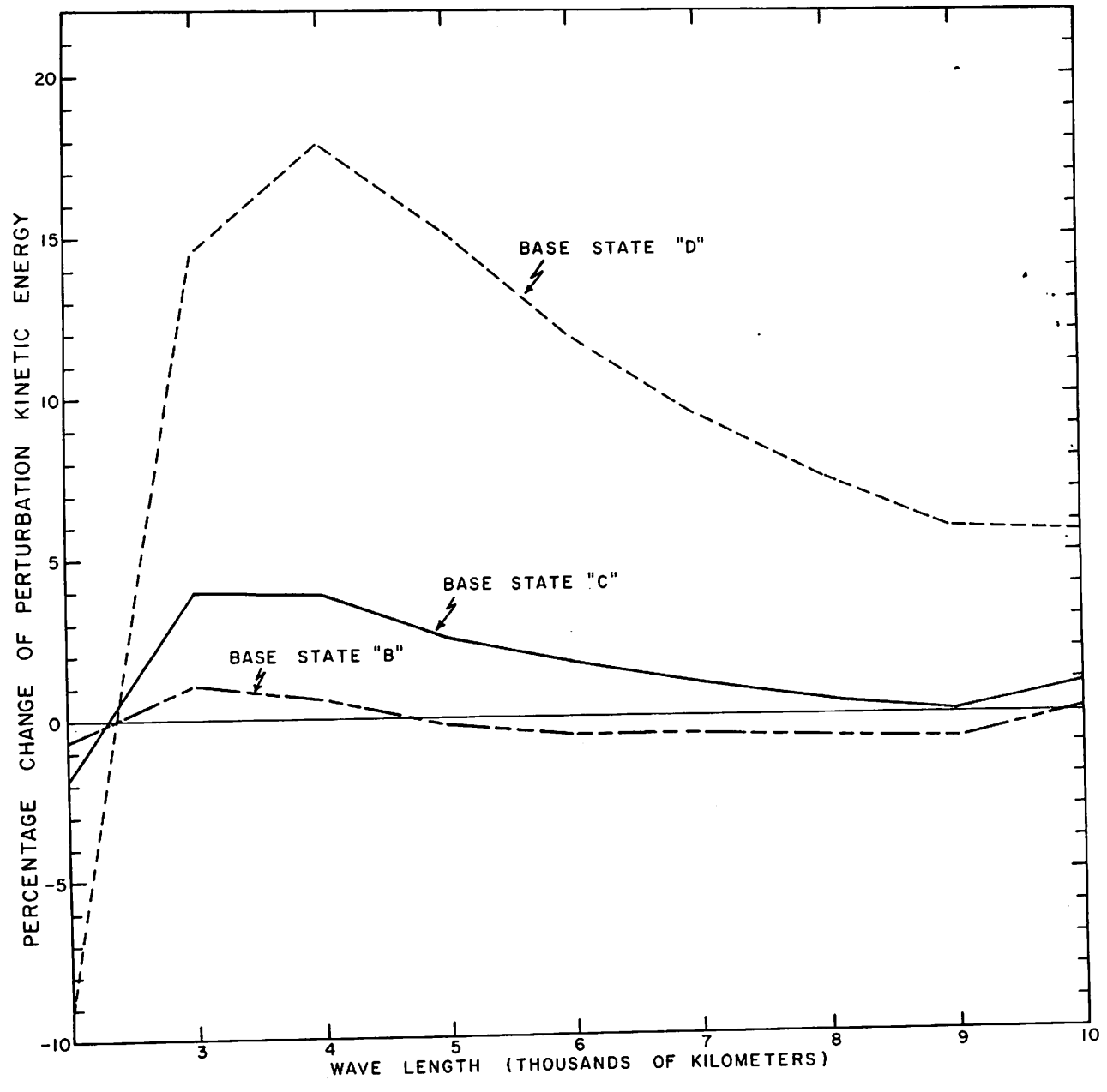


Figure 4. - Percentage change of perturbation kinetic energy over 48-hr. period as a function of wavelength for various base states.

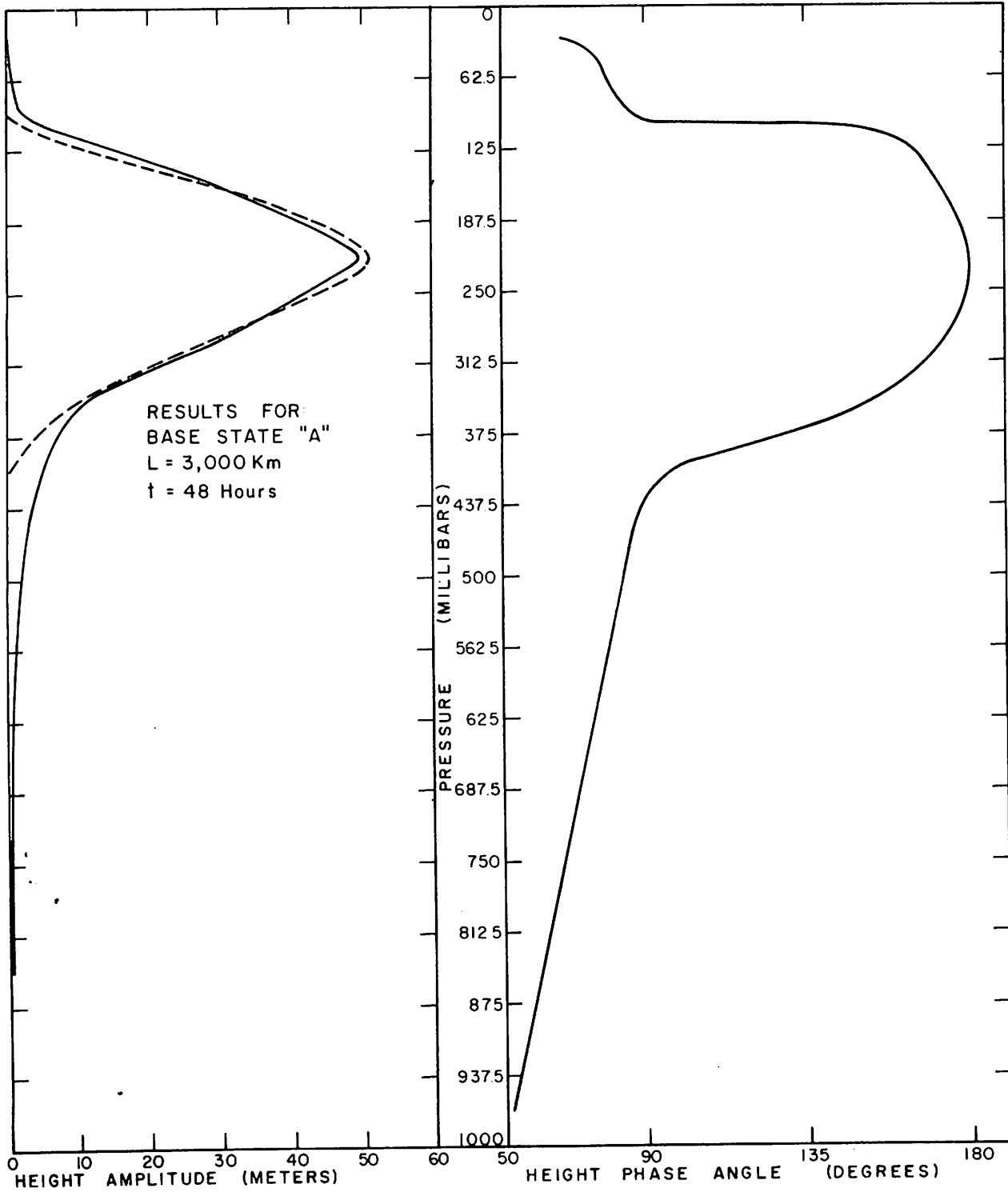


Figure 5. - Vertical profiles of z' -amplitude and z' -phase angle after 48 hr., Base State A, $L = 3000$ km. Phase-angle scale relative to positioning of 218.75-mb. trough at 180° .

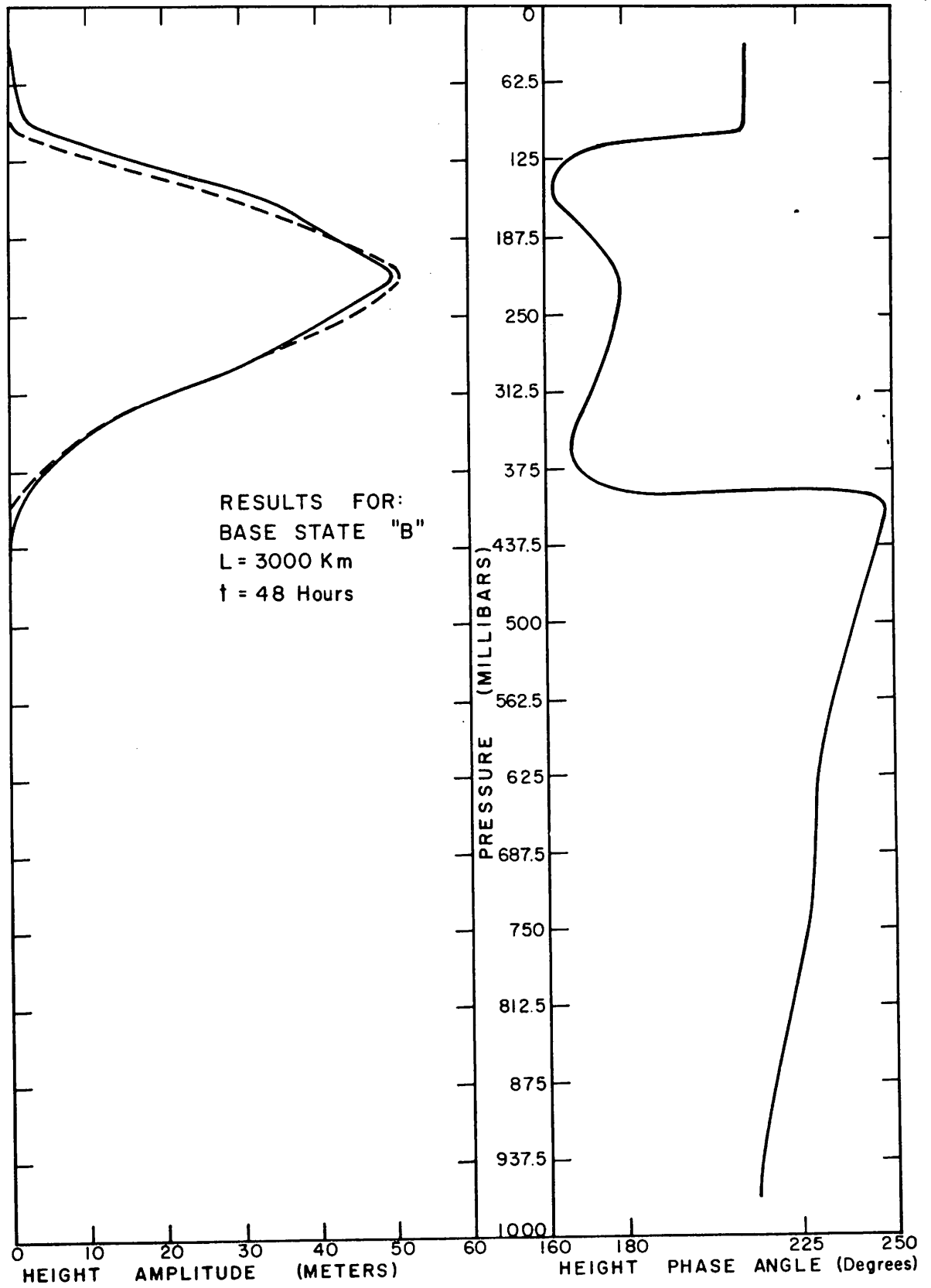


Figure 6. - Vertical profiles of z' -amplitude and z' -phase angle after 48 hr., Base State B, $L = 3000$ km. Phase-angle scale relative to positioning of 218.75-mb. trough at 180° .

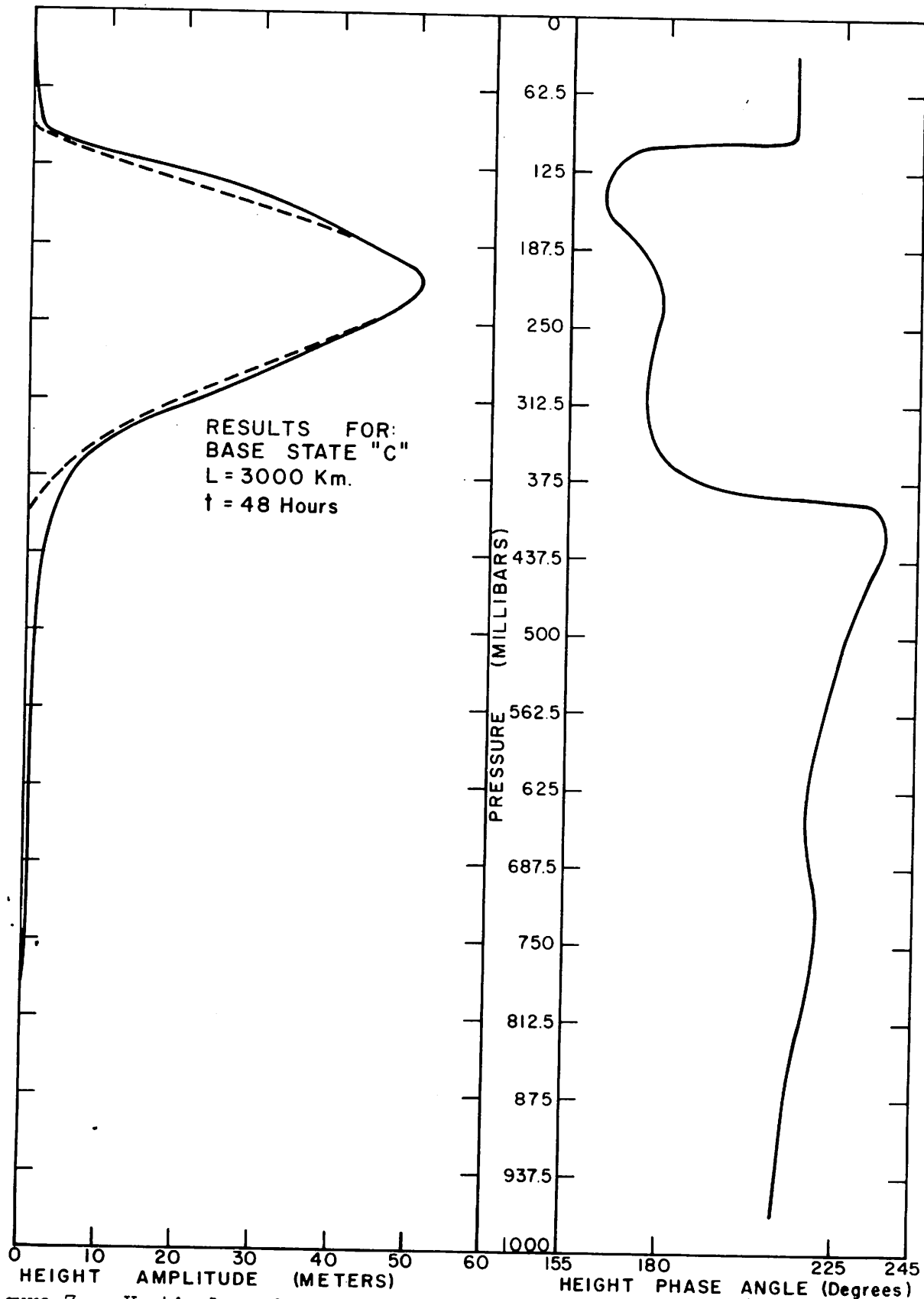


Figure 7. - Vertical profiles of z'-amplitude and z'-phase angle after 48 hr., Base State C, L = 3000 km. Phase-angle scale relative to positioning of 218.75-mb. trough at 180°.

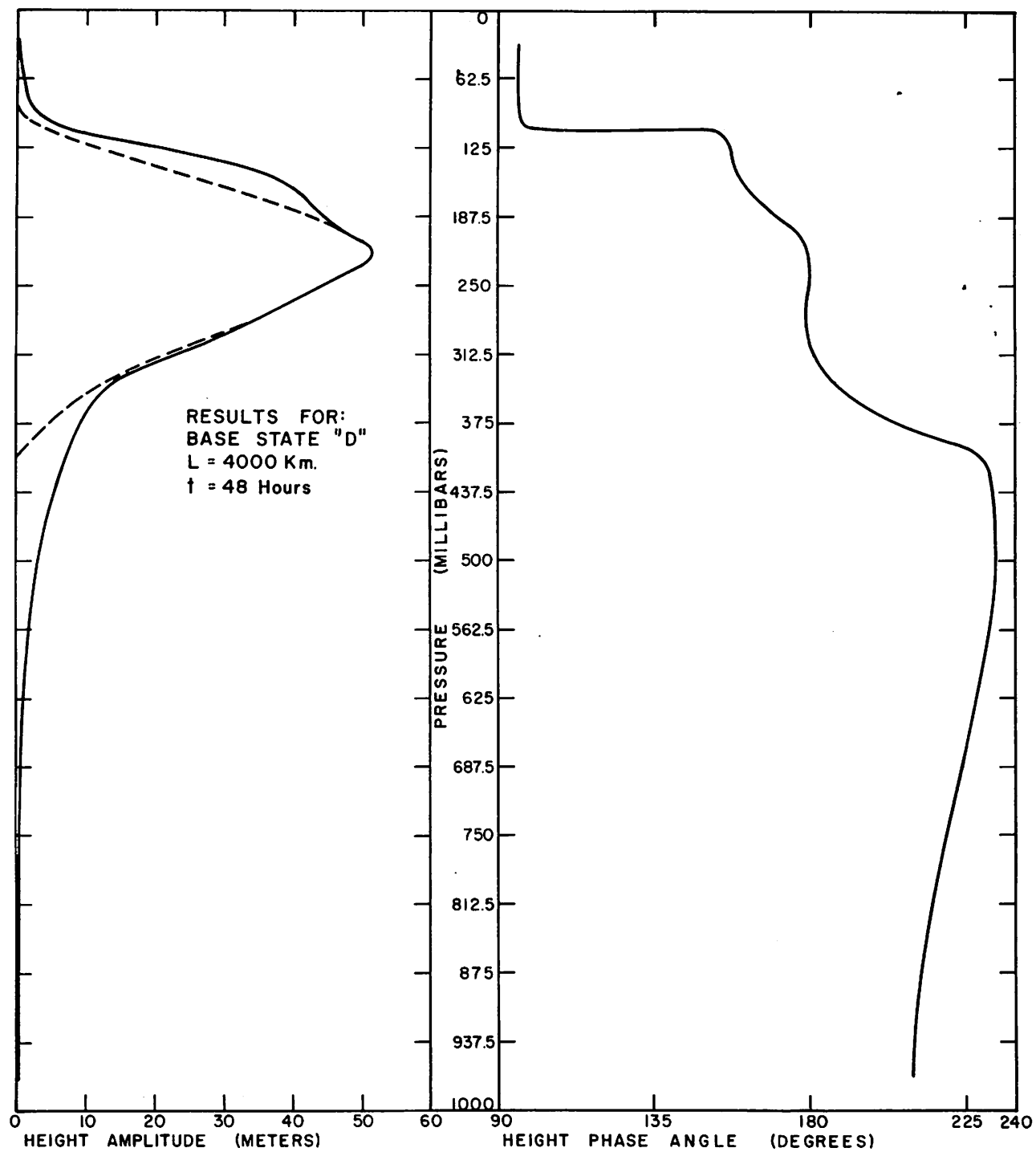


Figure 8. - Vertical profiles of z' -amplitude and z' -phase angle after 48 hr., Base State D, $L = 4000$ km. Phase-angle scale relative to positioning of 218.75-mb. trough at 180° .

Base States A and B (figs. 5 and 6, respectively) we actually find a slight decrease in the amplitude of the z' -perturbation at the level of maximum intensity.

On the basis of figures 4-8, we can conclude that there is no tendency for the theoretical perturbations to be damped rapidly, provided that L is 3000 km. or more. In the baroclinic cases, the $L = 2000$ km. disturbance does have a definite tendency to be damped. Stated in another way, our theoretical results do not support the contention that the upper-tropospheric vortex trains, in the observed wavelengths, are indirect circulations which would damp rapidly without an external source of kinetic energy.

Figure 9 is a zonal cross-section at 20° N. of the initial z' -perturbation. Figure 10 shows similar cross-sections of the initial ω' and divergence for Base State A, $L = 3000$ km. The vertical motion (fig. 10a) vanishes close to the level of maximum z' -amplitude. Below this level, upward motion takes place to the west of the trough and downward motion occurs to its east. The initial convergence-divergence pattern (fig. 10b) shows greatest intensity near the level of greatest z' -amplitude. Here, divergence occurs to the west of the trough and convergence to its east. Two surfaces of non-divergence are found. One of these is below the level of maximum-height amplitude while the other is above this level. Cross-sections of z' , ω' , and divergence, for the same base state and wavelength at 48 hr., are given by figure 11. While the trough and ridge lines now undulate through convergent and divergent regions, we find the trough (ridge) line to be weakly divergent (convergent) at the level of maximum z' -amplitude. This accounts for the decrease of z' -amplitude at this level which was noted earlier.

Figure 12 shows cross-sections of the initial vertical motion and divergence for Base State D, $L = 4000$ km. In this case, maximum vertical motion (and the only surface of nondivergence) occurs at 250 mb. The vertical motion vanishes only at the top and bottom of the atmosphere. Downward (upward) motion occurs to the west (east) of the trough line. The z' , ω' , and divergence patterns after 48 hr. are shown by figure 13. The trough (ridge) line is now convergent (divergent) at all levels. However, at the level of maximum z' -amplitude, the convergence (divergence) on the trough (ridge) line is extremely weak. At higher elevations, the trough (ridge) line shows considerably stronger convergence (divergence). This accounts for the substantial increase of z' -amplitude which was evident in the layer 187.5-125 mb. on figure 8.

4. CONCLUSIONS

The results of this study do not support the contention that the upper-tropospheric vortex trains are indirect circulations which require an external source of kinetic energy for their maintenance. On the other hand, our results also lend no support to the contention that these upper-level disturbances are produced by a baroclinic release of kinetic energy; in no case did we find the perturbation amplitude to increase at the level of maximum intensity. The conclusions discussed in the previous paragraph are considered to be preliminary. Work now in progress is aimed at improving the physical model. We also plan to carry out more complete tests for the purpose of determining the significance of slight variations in the initial conditions.

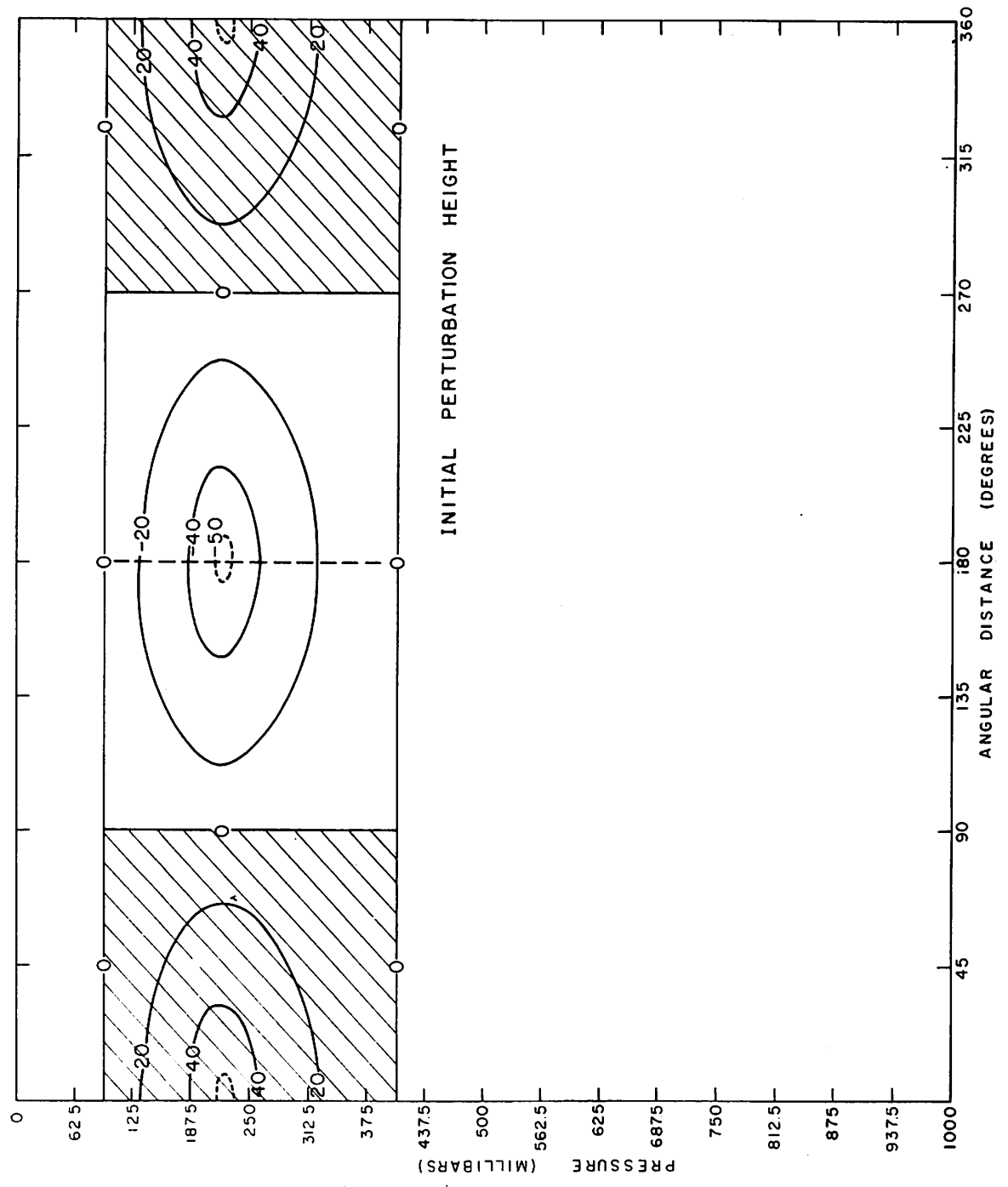


Figure 9. - Zonal cross-section of initial height perturbation at 20° lat. Units are m. sec.⁻¹

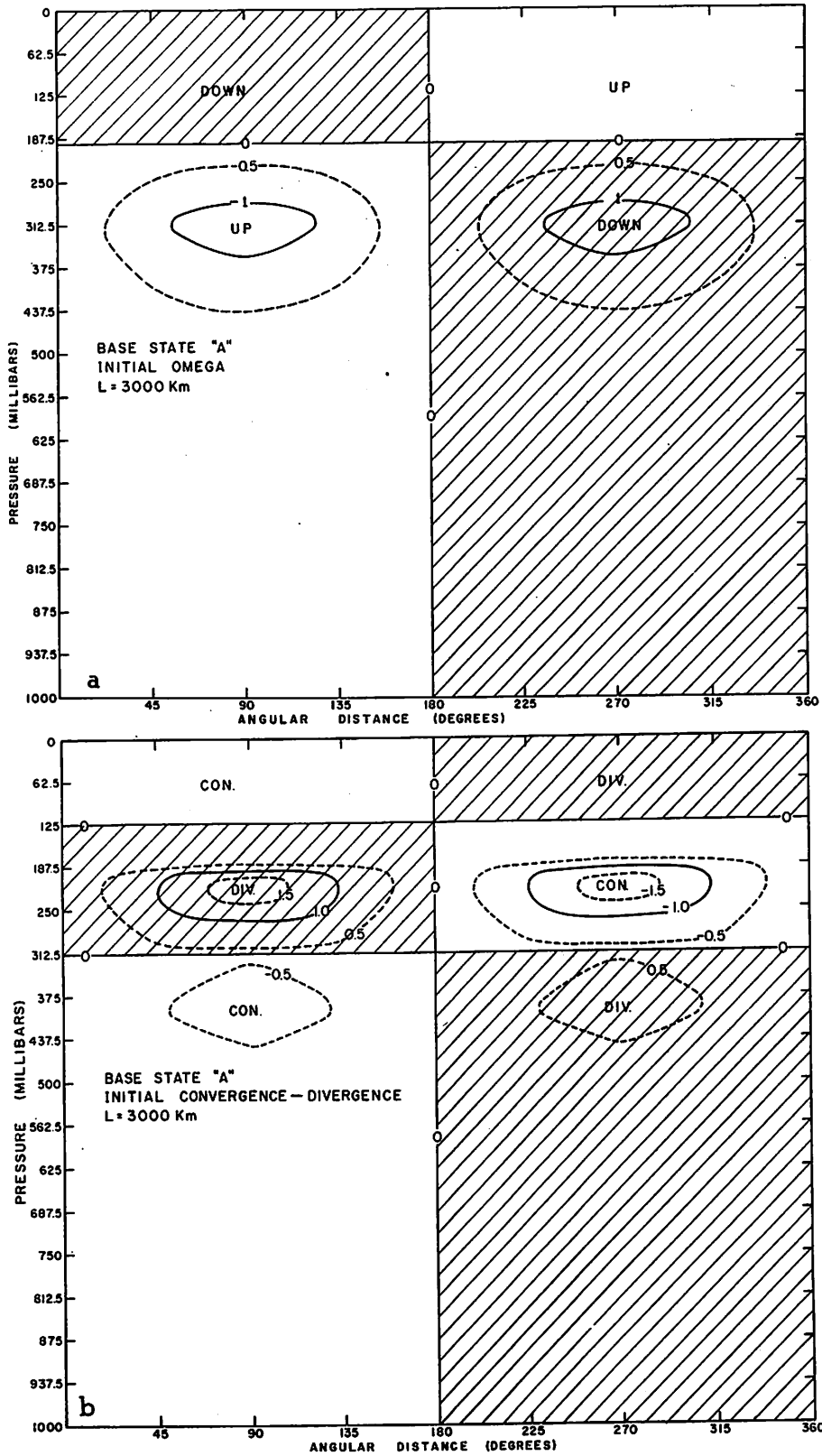


Figure 10. - Zonal cross-sections at 20° N., Base State A. L = 3000 km. (a) initial omega in units of 10^{-4} mb. sec.⁻¹, (b) initial divergence in units of 10^{-6} sec.⁻¹

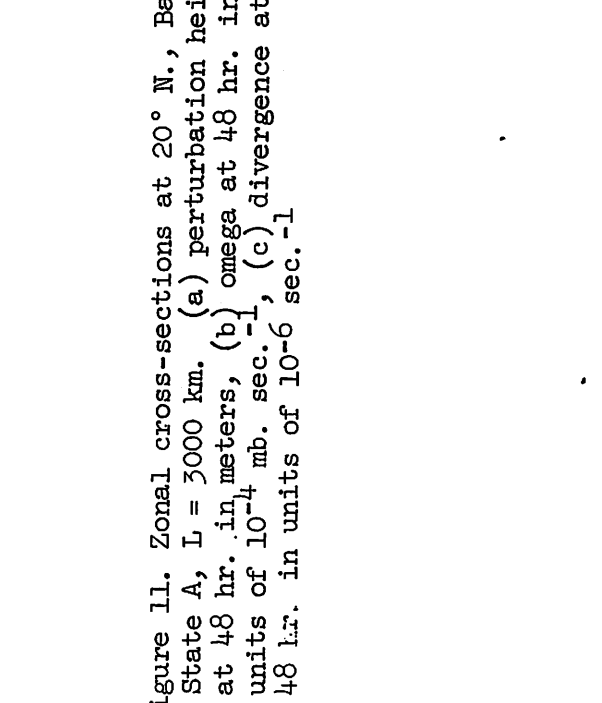
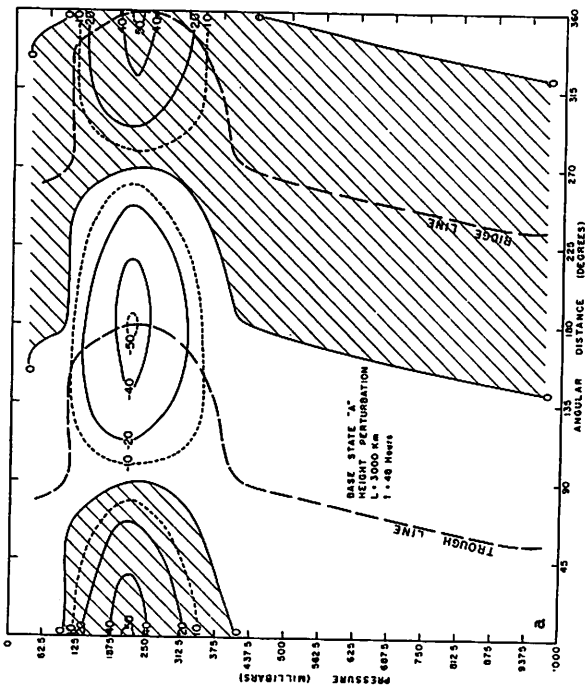
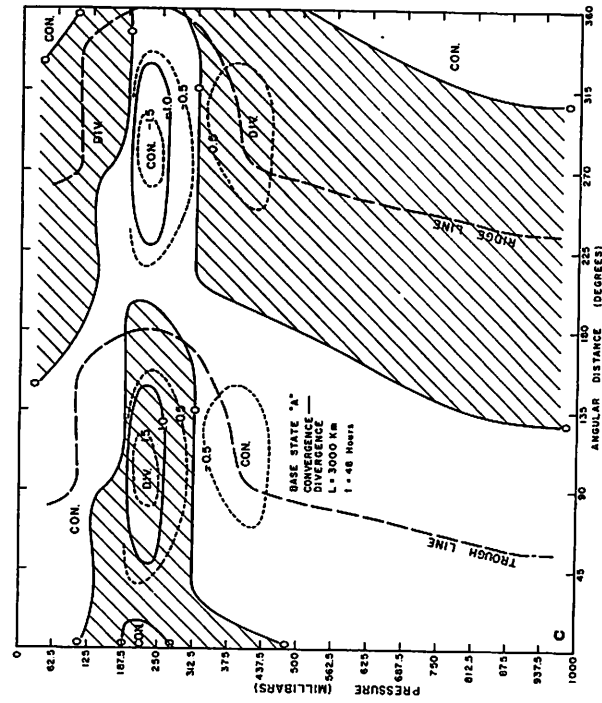


Figure 11. Zonal cross-sections at 20° N., Base State A, L = 3000 km. (a) perturbation height at 48 hr. in meters, (b) omega at 48 hr. in units of 10⁻⁴ mb. sec.⁻¹, (c) divergence at 48 hr. in units of 10⁻⁶ sec.⁻¹

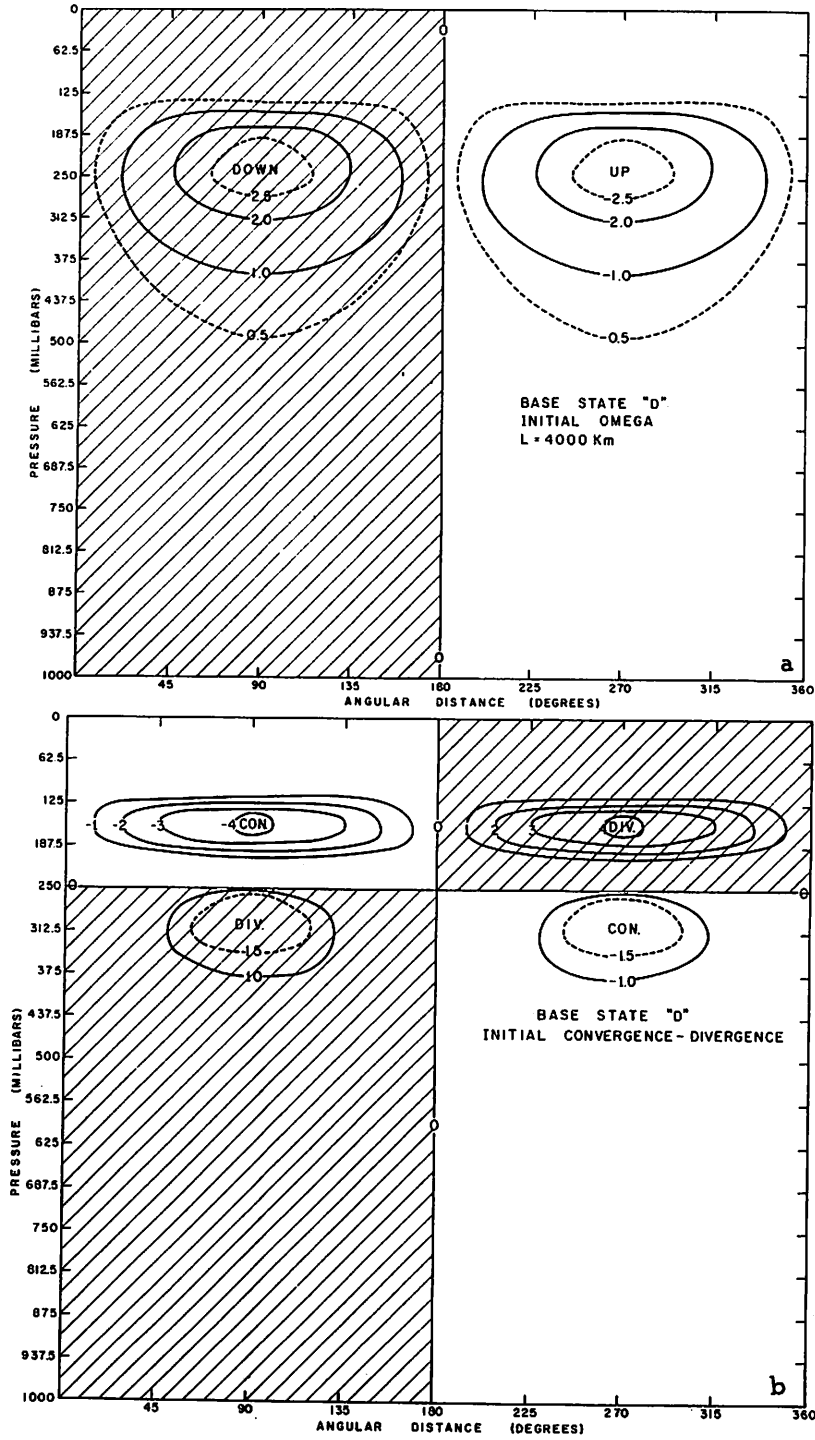


Figure 12. - Zonal cross-sections at 20°N., Base State D, L = 4000 km.
 (a) initial omega in units of 10^{-4} mb. sec. $^{-1}$ (b) initial divergence in units of 10^{-6} sec. $^{-1}$

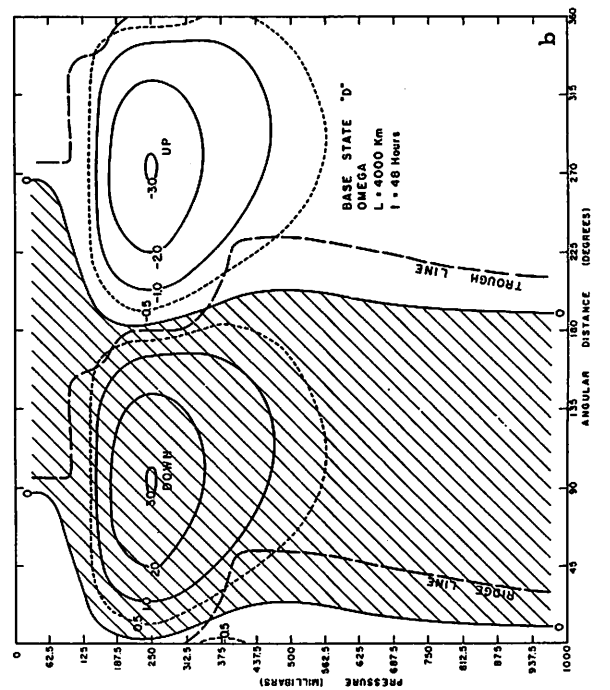
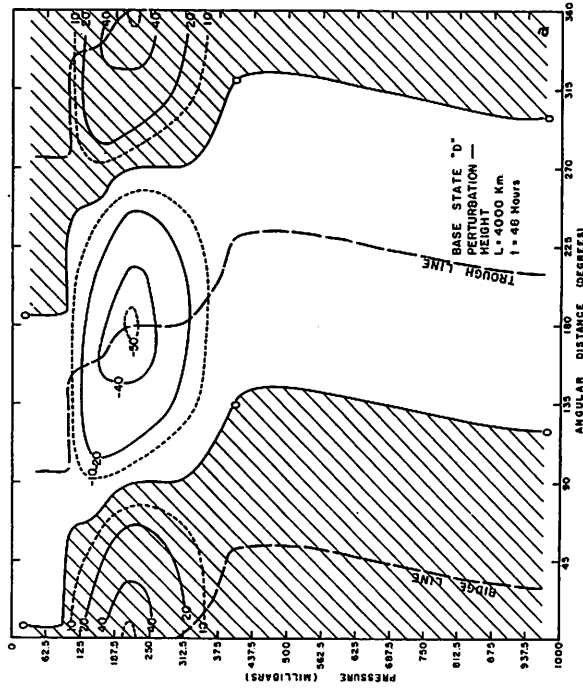
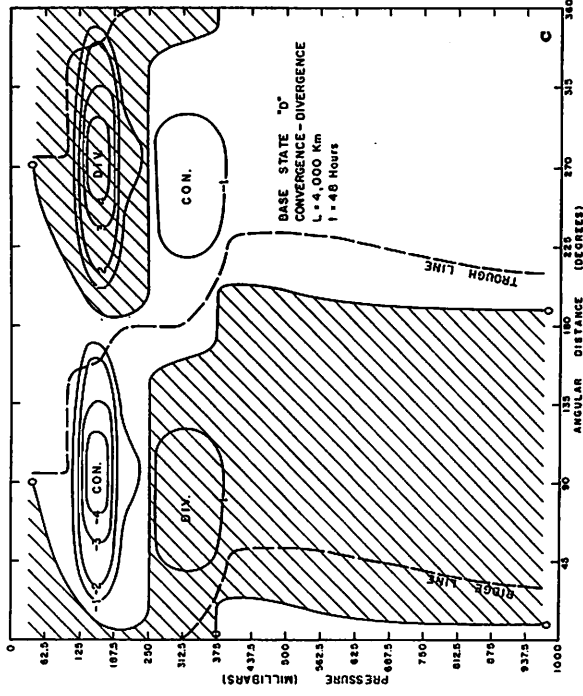


Figure 13. - Zonal cross-sections at 20° N., Base State D, L = 4000 km. (a) perturbation height at 48 hr, in meters, (b) omega at 48 hr. in units of 10⁻⁴ mb. sec.⁻¹, (c) divergence at 48 hr. in units of 10⁻⁶ sec.⁻¹

ACKNOWLEDGMENT

The author is indebted to his colleagues, Harry F. Hawkins, Banner I. Miller, Walter J. Koss, and M. A. Lateef for providing critical reviews of the manuscript. James W. Trout assisted in the machine coding of the problem.

REFERENCES

1. A. Arakawa, "Non-Geostrophic Effects in the Baroclinic Prognostic Equations," Proceedings of the International Symposium on Numerical Weather Prediction in Tokyo, Nov. 7-13, 1960, The Meteorological Society of Japan, Tokyo, 1962, pp. 161-175.
2. J. Charney, "A Note on Large-Scale Motions in the Tropics," Journal of the Atmospheric Sciences, vol. 20, No. 6, Nov. 1963, pp. 607-609.
3. J. Charney, "The Use of the Primitive Equations of Motion in Numerical Prediction," Tellus, vol. 7, No. 1, Feb. 1955, pp. 22-26.
4. H. U. Groening, "Wind and Pressure Fields in the Stratosphere over the West Indies Region in August 1958," National Hurricane Research Project Report No. 35, U. S. Weather Bureau, 1959, 10 pp.
5. L. F. Hubert, "High Tropospheric Westerlies of the Equatorial West Pacific Ocean," Journal of Meteorology, vol. 6, No. 3, June 1949, pp. 216-224.
6. C. L. Jordan, "An Experiment in Low-Latitude Numerical Prediction with the Barotropic Model," Journal of Meteorology, vol. 13, No. 3, June 1956, pp. 223-235.
7. C. L. Jordan, "Mean Soundings for the West Indies Area," Journal of Meteorology, vol. 15, No. 1, Feb. 1958, pp. 91-97.
8. N. E. LaSeur, "Tropical Synoptic Models - A Survey," paper presented at Symposium on Tropical Meteorology, November 1963, Rotorua, New Zealand.
9. W. E. Milne, Numerical Solution of Differential Equations, Wiley and Sons, New York, 1953, 275 pp.
10. C. E. Palmer, "On High-Level Cyclones Originating in the Tropics," Transactions of the American Geophysical Union, vol. 32, No. 5, Oct. 1951, pp. 683-695.
11. C. E. Palmer, "Tropical Meteorology," Quarterly Journal of the Royal Meteorological Society, vol. 78, No. 336, Apr. 1952, pp. 126-163.
12. C. S. Ramage, "The Subtropical Cyclone," Scientific Report No. 1, under Contract AF19(604)-6156, Institute of Geophysics, University of Hawaii, 1961, 26 pp.
13. R. D. Richtmyer, Difference Methods for Initial Value Problems, Interscience Publishers, New York, 1957, 238 pp.

14. R. L. Ricks, "On the Structure and Maintenance of High-Tropospheric Cold-Core Cyclones of the Tropics," Master of Science dissertation, Dept. of Meteorology, The University of Chicago, Chicago, Ill., 1959, 32 pp.
15. H. Riehl, "On the Formation of Typhoons," Journal of Meteorology, vol. 5, No. 6, Dec. 1948, pp. 247-264.
16. H. Riehl, "On the Production of Kinetic Energy from Condensation Heating," The Atmosphere and the Sea in Motion, Rockefeller Institute Press with Oxford University Press, New York, 1959, pp. 381-399.
17. H. Riehl, Tropical Meteorology, McGraw-Hill Book Co., Inc., New York, 1954, 392 pp.
18. R. H. Simpson, "Evolution of the Kona Storm, a Subtropical Cyclone," Journal of Meteorology, vol. 9, No. 1, Feb. 1952, pp. 24-35.
19. A. Wiin-Nielsen, "On Truncation Errors due to Vertical Differences in Various Numerical Prediction Models," Tellus, vol. 14, No. 3, Aug. 1962, pp. 261-280.
20. M. Yanai, "Dynamical Aspects of Typhoon Formation," Journal of Meteorological Society of Japan, Series II, vol. 39, No. 5, Oct. 1961, pp. 282-309.

APPENDIX

The finite difference grid is described by table 2. Equations (16) and (17) were approximated by

$$\left(\frac{C_{i+2} - 2C_i + C_{i-2}}{4\Delta p^2}\right) - \sigma_i \left(\frac{n}{f_0}\right)^2 C_i = 2k \left(\frac{n}{f_0}\right)^2 \left(\frac{U_{i+1} - U_{i-1}}{2\Delta p}\right) B_i - \frac{\beta k}{f_0^2} \left(\frac{B_{i+1} - B_{i-1}}{2\Delta p}\right)$$

$$\left(\frac{D_{i+2} - 2D_i + D_{i-2}}{4\Delta p^2}\right) - \sigma_i \left(\frac{n}{f_0}\right)^2 D_i = -2k \left(\frac{n}{f_0}\right)^2 \left(\frac{U_{i+1} - U_{i-1}}{2\Delta p}\right) A_i + \frac{\beta k}{f_0^2} \left(\frac{A_{i+1} - A_{i-1}}{2\Delta p}\right)$$

which may be arranged to read

$$C_{i+2} - [2 + 4\sigma_i \left(\frac{n\Delta p}{f_0}\right)^2] C_i + C_{i-2} = 4k\Delta p \left(\frac{n}{f_0}\right)^2 (U_{i+1} - U_{i-1}) B_i - \frac{2\beta k\Delta p}{f_0^2} (B_{i+1} - B_{i-1})$$

$$D_{i+2} - [2 + 4\sigma_i \left(\frac{n\Delta p}{f_0}\right)^2] D_i + D_{i-2} = -4k\Delta p \left(\frac{n}{f_0}\right)^2 (U_{i+1} - U_{i-1}) A_i + \frac{2\beta k\Delta p}{f_0^2} (A_{i+1} - A_{i-1})$$

$$i = 1, 3, 5, 7, \dots, 31.$$

The pressure increment, Δp , is 31.25 mb. These difference equations were solved for C and D at the internal odd points by Richtmyer's method ([13] p. 102). For the even points,

$$C_i = \frac{C_{i+1} + C_{i-1}}{2}, \quad D_i = \frac{D_{i+1} + D_{i-1}}{2}, \quad i = 2, 4, 6, \dots, 32$$

The prognostic relationships, (14) and (15), were approximated by

$$\frac{\partial A_i}{\partial t} = kC_{R_i} B_i - \left(\frac{f_0}{n}\right)^2 \left(\frac{C_{i+1} - C_{i-1}}{2\Delta p}\right)$$

and

$$\frac{\partial B_i}{\partial t} = -kC_{R_i} A_i - \left(\frac{f_0}{n}\right)^2 \left(\frac{D_{i+1} - D_{i-1}}{2\Delta p}\right)$$

$$i = 2, 4, 6, \dots, 32.$$

The time integrations were performed by use of Milne's iterative technique ([9] p. 25). Time steps of 1/2 hour were employed. At each time step, the iterative process was terminated only after A and B had been stabilized to within $10^{-2} \text{ m.}^2 \text{ sec.}^{-2}$. Finally, at the odd interior points,

$$A_i = \frac{A_{i+1} + A_{i-1}}{2}, \quad B_i = \frac{B_{i+1} + B_{i-1}}{2}, \quad i = 3, 5, 7, \dots, 31.$$

As a practical check on truncation error, the value of K at 48 hr., as computed from equation (21), was compared with the value given by a numerical integration of equation (24) using the half-hourly values of A, B, C, and D. Discrepancies between the two K-values were negligible in comparison with the 48-hr. changes of either.

Table 2. Description of finite difference grid.

Grid-Point Index	Grid-Point Pressure(mb.)	Equation Applied
1	0	
2	31.25	vorticity
3	62.50	omega
4	93.75	vorticity
5	125.00	omega
6	156.25	vorticity
7	187.50	omega
8	218.75	vorticity
9	250.00	omega
10	281.25	vorticity
11	312.50	omega
12	343.75	vorticity
13	375.00	omega
14	406.25	vorticity
15	437.50	omega
16	468.75	vorticity
17	500.00	omega
18	531.25	vorticity
19	562.50	omega
20	593.75	vorticity
21	625.00	omega
22	656.25	vorticity
23	687.50	omega
24	718.75	vorticity
25	750.00	omega
26	781.25	vorticity
27	812.50	omega
28	843.75	vorticity
29	875.00	omega
30	906.25	vorticity
31	937.50	omega
32	968.75	vorticity
33	1000	